EVALUATIONS OF INEXTENSIBLE (MORE RIGID) AND EXTENSIBLE (LESS RIGID) GRID REINFORCEMENTS IN INFRASTRUCTURE PROJECTS ON SOFT BANGKOK CLAY

D.T.Bergado | Associate Professor of Geotechnical Engineering, School of Civil Engineering, Asian Institute of Technology

N.Miura | Dean, Faculty of Science and Engineering, Saga University

M.C.Alfaro | Doctoral Student, Department of Civil Engineering, Saga University

Abstract

This paper contains the evaluations regarding the performances of grid reinforcements with different stiffness under full scale loading conditions on soft Bangkok clay. Two reinforced test embankments were constructed to about 6.0m high with vertical facing, one with steel grid reinforcements (higher rigidity) and the other with polymer geogrid reinforcements (lower rigidity). The results indicate that increasing the rigidity of the reinforced mass tends to increase the settlement under the toe or under the face of the reinforced wall due to its rigid body rotation. Moreover, increasing the reinforcement rigidity tends to decrease the lateral spreading of the foundation subsoil. Furthermore, higher shear stress concentrations were observed under the toe or under the wall face of the steel grids reinforced wall (higher rigidity) signifying further the rigid body rotation. Both reinforced walls registered larger tension forces in the reinforcement layers near the base of the test embankments caused by the bending action resulting from the bowl-shaped differential settlements. The locations of the maximum tensile forces in the facilities were found to be nearer to the wall face than those normally assumed for reinforced structures resting on competent foundations. Finally, the presence of weathered crust in the subsoil near the ground surface affects very much the effects of the reinforcements on the stability of reinforced structures.

1. Introduction

The important coastal areas where the major cities are located in Southeast Asian region are shown in Fig. 1. In coastal areas, the main foundation problem is the presence of thick and soft clay deposits which is very weak and compressible material with associated low bearing capacity, large settlements, and slope instability. Another problem is the phenomenon of lateral spreading that will contribute to total and differential settlements. The construction of reinforced structures, tend to hold against the outward thrust minimizing the lateral spreading. In addition, the beneficial effects of earth reinforcements results in

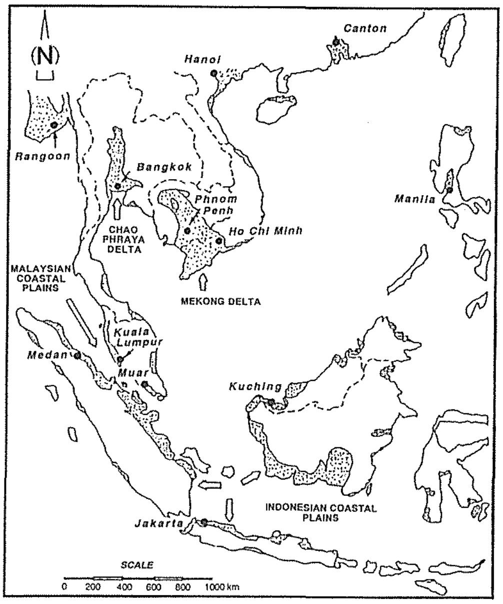

Fig. 1 Soft Clay Deposits of Southeast Asia

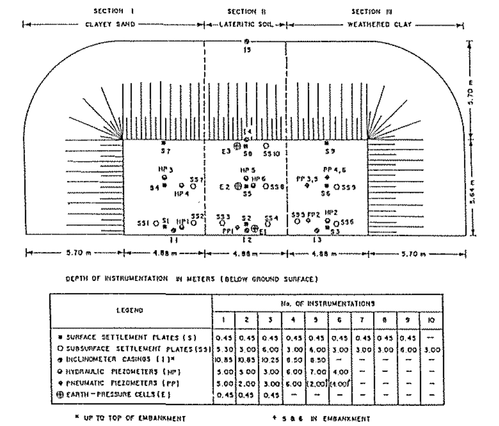

(a)

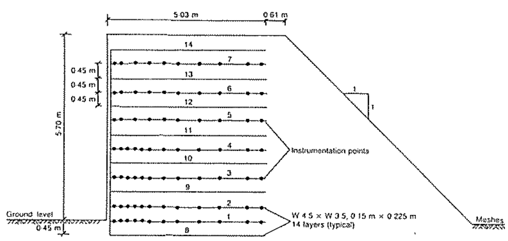

(b)

Fig. 2a Layout of Field Instrumentation for Test Facility I
2b Reinforcement Instrumentation for Test Facility I

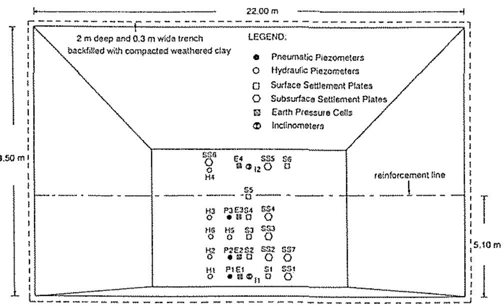

(a)

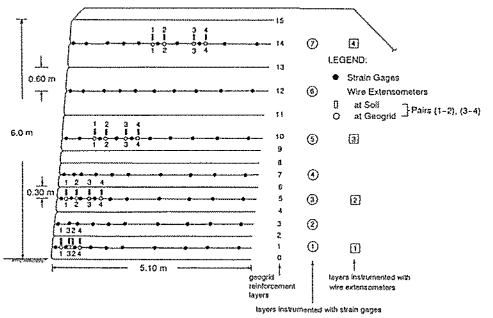

(b)

Fig. 3a Layout of Foundation Instrumentation of Test Facility II
3b Strain Measurements on Geogrid Reinforcement and Backfill Soil at Test Facility II

increased stability and bearing capacity.

Two full scale test embankments were constructed on soft Bangkok clay using steel grid reinforcements in one and polymer geogrid reinforcements in the other, hereinafter termed Facility I (Fig. 2a,b) and Facility II (Fig. 3a,b), respectively. The steel grids represents higher rigidity and higher strength with about 100kN/m yield strength. The polymer geogrid signify lower rigidity and lower tensile strength with about 45kN/m strength at break. Both facilities have the same backfill materials consisting of compacted weathered Bangkok clay whose properties are given in Table 1 with maximum standard Proctor compacted dry density of 16 kN/m^3 and optimum moisture content of 22%. The soil profile together with the soil properties are given in Fig. 4. The properties of the soft Bangkok clay subsoils are given in Table 2. Additional subsoils properties are plotted with depth in Fig. 5. Typical instrumentations of the embankment are laid out in Fig. 6. The main points of comparison are focused on the different behavior of test facilities such as: lateral deformations, foundation differential settlements, vertical base pressures, tensile forces in the reinforcements, stress concentrations in the foundation subsoils, and the effect of the uppermost weathered crust layer in the foundation subsoils.

Table 1 Summary of Backfill Soil Properties

Soil	G_s	W_P	W_L	I_p	Passing sieve number 200 (0.075mm)	W_{opt}	γ_{dmax}	Direct Shear		Unconsolidated Undrained		Isotropically Consolidated Undrained			
								C	ϕ	C	ϕ	C	ϕ	C	ϕ
		%	%	%	%	%	kN/m^3	kN/m^2	Degrees	kN/m^2	Degrees	kN/m^2	Degrees	kN/m^2	Degrees
Weathered clay	2.67	21	45	24	82.94	22	16.3	129	30.7	118	31.5	19	25.8	24	15.5

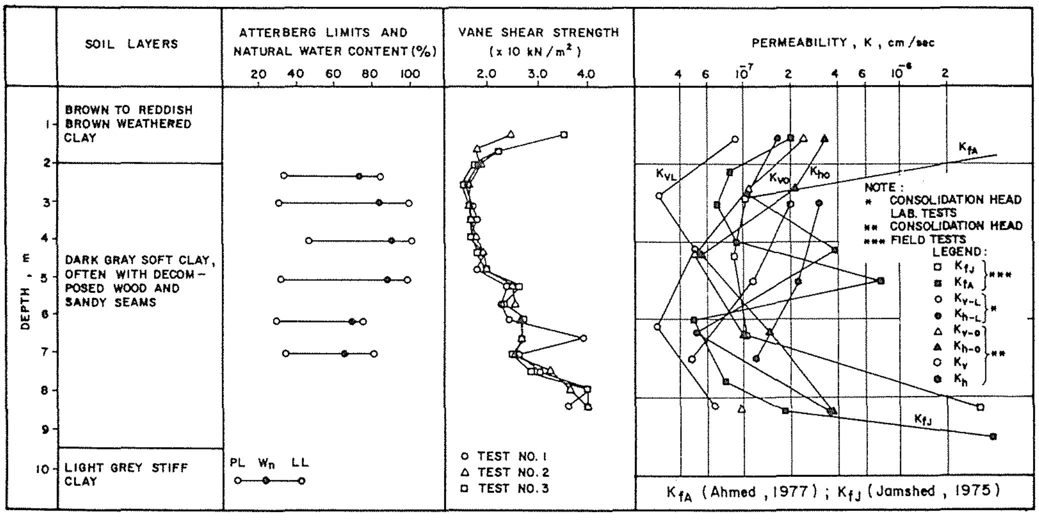

Fig. 4 Soil Profile and Properties at Site

Table 2 Soil Parameters of Soft Bangkok Clay

Parameter	Symbol	1 0-1m	2 1-2m	3 2-6m	4 6-8m	5 8-12m
Kappa	κ		0.04	0.11	0.07	0.04
Lambda	λ		0.18	0.51	0.31	0.18
C.S.L.Slope	M		1.10	0.90	0.95	1.10
Gamma	Γ		3.00	5.12	4.00	2.90
Poisson's Ratio	ν	0.25	0.25	0.30	0.30	0.25
Modulus (kPa)	E	4000				
Friction Angle (^{0})	ϕ'	29.0				
Cohesion (kPa)	c'	29.0				
Unit Weight (kN/m^3)	γ	17.5	17.5	15.0	16.5	17.5
Horizontal Permeability (m/sec), (x10^{-8})	k_h	34.7	34.7	5.2	5.2	34.7
Vertical Permeability (m/sec), (x10^{-8})	k_v	17.4	17.4	2.6	2.6	17.4

Note: k_v=25 times of estimated average laboratory test value
k_h=2 times of the k_v

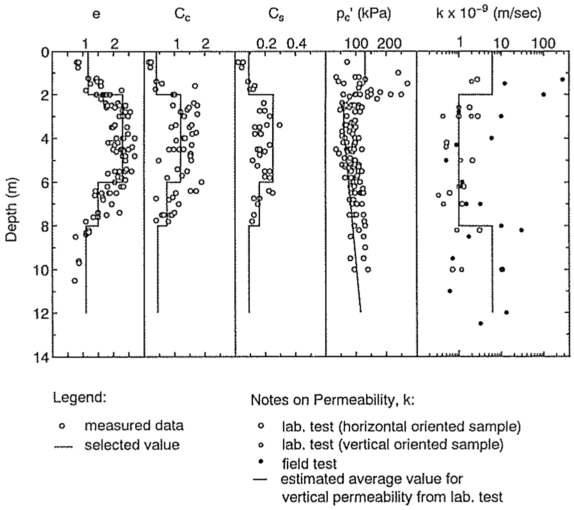

Fig. 5 Additional Soil Properties with Depth

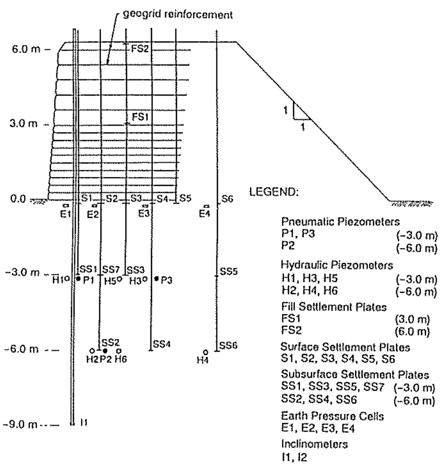

Fig. 6 Instrumented Section of Test Facility II

2. Lateral Deformations

The lateral deformations of the two test facilities during construction and post construction periods are shown in Fig. 7. The inclinometer readings indicated that the lateral deformation occurred mainly between 3 to 5m depth below the ground surface coinciding with the weakest part of the foundation soil. As shown in Fig. 7, the inclinometer at Test Facility I (with inextensible reinforcements) was damaged so that monitoring at greater depths was not possible 8 months after construction.

The maximum outward lateral deformation of the test facilities occurred at the top of the wall face. At the end of construction, the test facility with extensible reinforcement has slightly higher lateral movement compared to that with inextensible reinforcements. These differences are blamed on the different methods of construction.

The post construction deformations, however, indicates that Test Facility I with inextensible reinforcements registered higher lateral movement at the top of the wall face than Test Facility II. This behavior can be explained by the tilting forward of Test Facility I due to rigid body rotation caused by the unequal compression of the soft clay foundation.

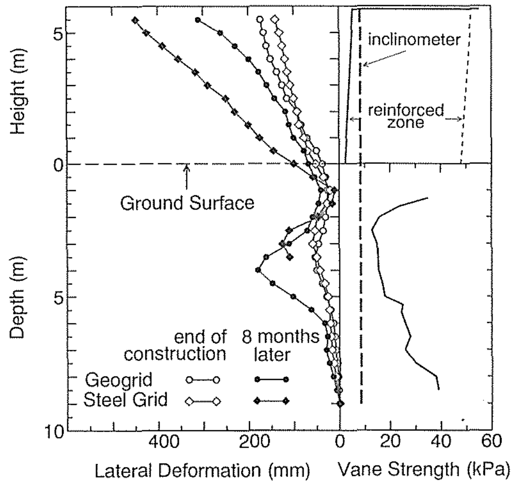

Fig. 7 Measured Lateral Deformations of the Two Test Facilities

The lateral movements in the foundation subsoil, reveals that the inextensible reinforcements of Test Facility I was able to reduce the lateral movements compared to that of Test Facility II. The former has greater system stiffness than the latter by more than sixty times as obtained by the following equation:

$$S_r = \frac{E \cdot A}{S_v \cdot S_h} \tag{1}$$

where S_r = reinforced soil system stiffness; E = Young's modulus (stiffness) of the reinforcement; A = cross-sectional area of the reinforcement; S_v = vertical reinforcement spacing; and S_h = horizontal reinforcement spacing.

3. Foundation Differential Settlements

The rate of foundation settlements at the toe and center of both test facilities are laid out in Fig. 8a,b. The settlement behavior initially have higher rates and then slowed down thereafter. Both test facilities have identical settlement characteristics at the center. However, at the toe beneath the wall face, the Test Facility I have higher settlement magnitude. The settlement profile below the

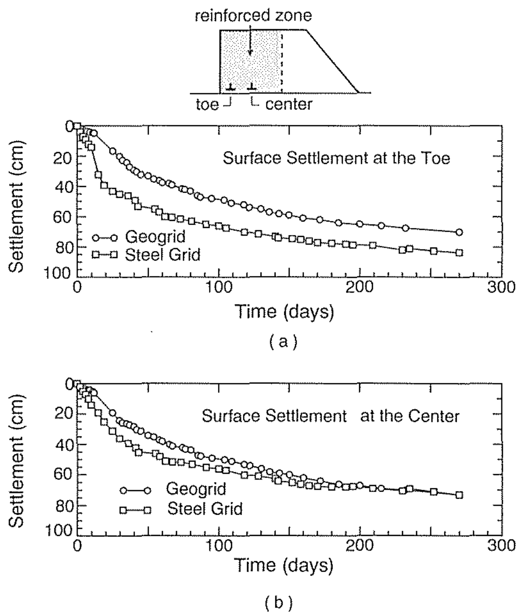

Fig. 8a,b Measured Foundation Settlement-Time History of the Two Test Facilities

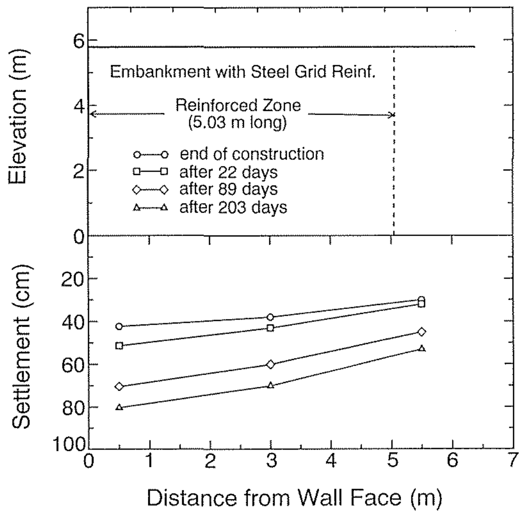

Fig. 9 Measured Foundation Settlement Profile Below the Reinforced Soil Mass at Test Facility I

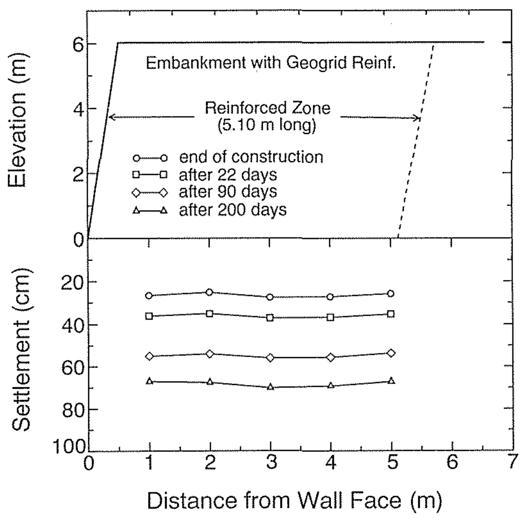

Fig. 10 Measured Foundation Settlement Profile Below the Reinforced Soil Mass at Test Facility II

reinforced mass of Test Facilities I and II are plotted in Figs. 9 and 10, respectively. While there is uniform settlement beneath Test Facility II, more settlements were observed below the toe than beneath the center of Facility I. This confilms the higher stiffness and higher rigidity of Test Facility I. A more rigid reinforced mass tends to rotate about the toe due to lateral thrust from behind. Most of the lateral movements at the top of the wall face Test Facility I (Fig. 7) can be explained by this rotational phenomenon of the more rigid reinforced mass (Alfaro, 1994).

4. Vertical Base Pressures

The observed vertical pressure distributions measured from total earth pressure cells are plotted in Fig. 11 a,b for both test facilities. Also shown are the results of using the three common assumptions for estimating vertical base pressures, namely: uniform, trapezoidal, and Meyerhof. The vertical base pressure close to the wall facing is generally less than the other locations. This maybe attributed to higher frictional resistance of the fill and facing interface. The effect of facing rigidity may have

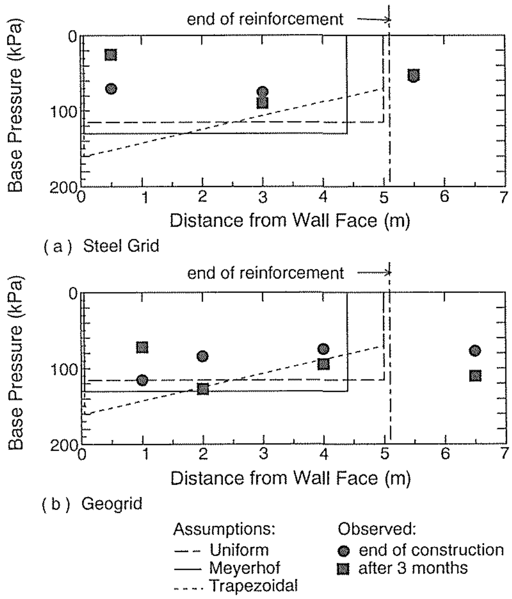

Fig. 11 a,b Measured Distribution of Vertical Base Pressures for the Two Test Facilities also reduced the vertical soil stress in the vicinity of the toe (Tasuoka, 1992). This behavior is also explained by the arching effects due to the interconnection of the wall facing elements (Bergado et al., 1991).

5. Tensile Forces in the Reinforcements

The tensile forces in the reinforcements were back-calculated from the measured strains. Figures 12 and 13 show the variations of tensile forces during both the construction and post construction periods of Test Facilities I and II, respectively. Also indicated in these figures are the assumed locations of maximum tensile forces established by both coherent gravity and tie-back wedge analyses. The observed maximum tensile forces were neither defined by these two assumptions. Instead, the location of maximum tensile forces tends to be closer to the wall face (dashed lines). This behavior is blamed on the compression of the soft clay foundation. Due to the bowl-shaped differential settlements, the tensile forces observed at the reinforcement near the base of the reinforced mass tend to be higher.

6. FEM Analyses

FEM analyses was done using CRISP computer software. Figures 14 a,b,c and 15 a,b,c show the deformation of FEM mesh for both facilities. The tilting forward of Test Facility I is clearly indicated. The shear stress distributions on both test

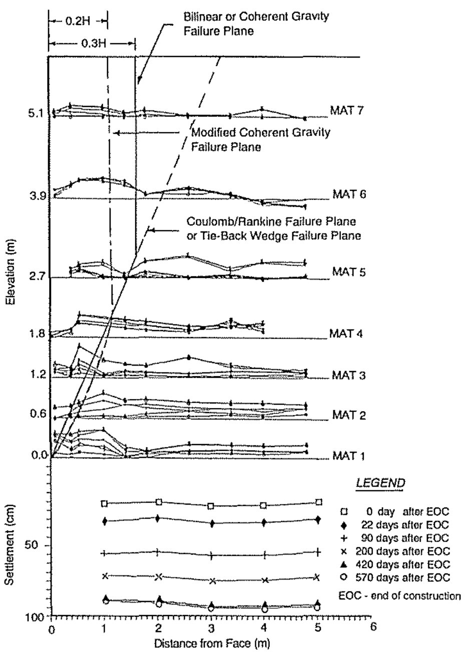

Fig. 12 Tensile Forces Distributions in the Reinforcement at Test Facility I

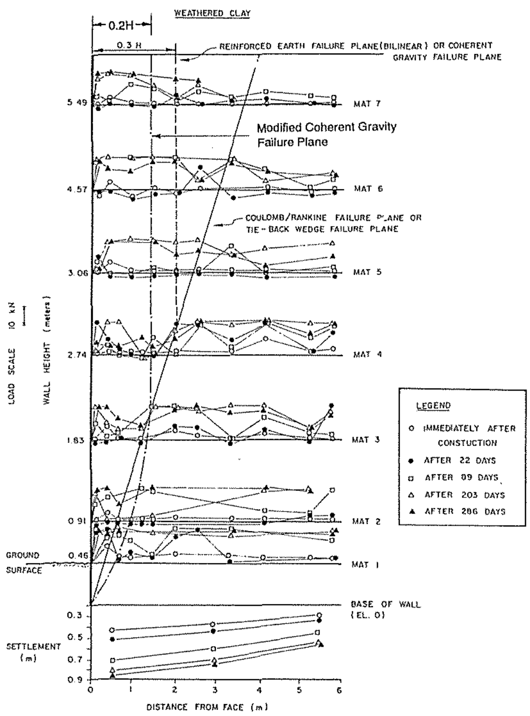

Fig. 13 Tensile Forces Distributions in the Reinforcement at Test Facility II

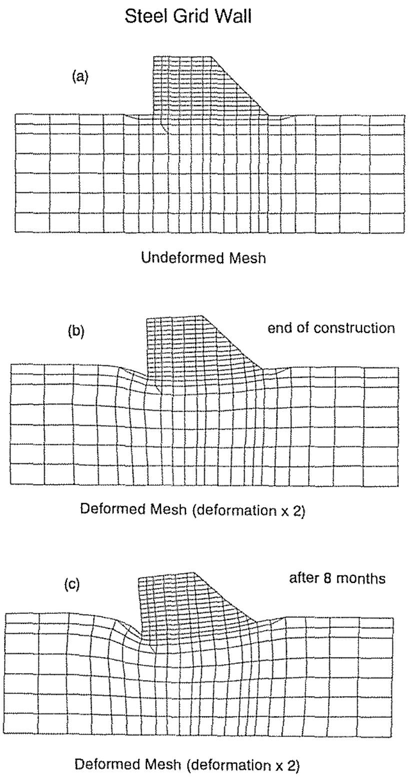

Fig. 14a,b,c Undeformed and Deformed FEM Mesh for Test Facility Ⅰ

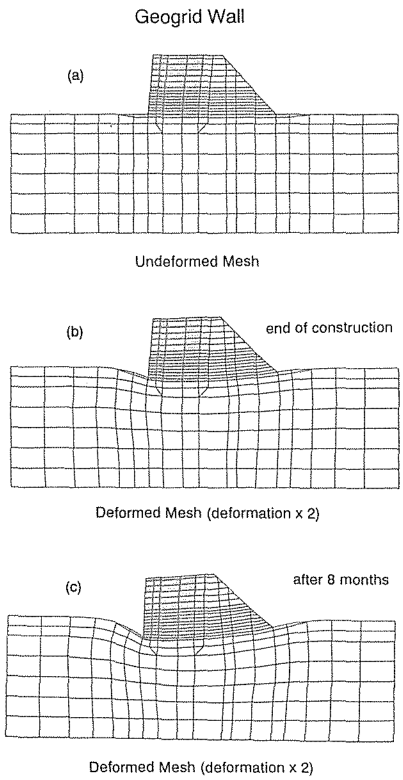

Fig. 15a,b,c Undeformed and Deformed FEM Mesh for Test Facility Ⅱ

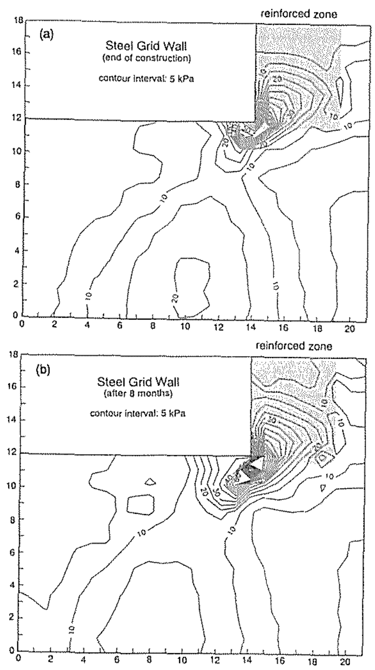

Fig. 16a,b Shear Stress Distribution Contours for Test Facility Ⅰ

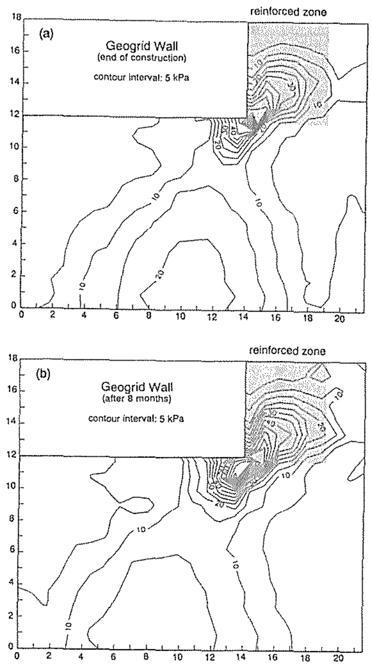

Fig. 17a,b Shear Stress Distribution Contours for Test Facility Ⅱ facilities are plotted in Figs. 16 a,b and 17 a,b. The shear stress distribution contours indicated higher stress concentration at the toe of Test Facility I confirming the rigid body rotation especially at 8 months after construction. On the other hand, the shear

Table 3 Summary of the Factor of Safety for HGE Embankment Stability Analysis with its Corresponding Assumed Undrained Shear Strength Distribution (By STABL6 software)

Type of Undrained Strength Used for Stability Analysis	If	γ (m)	Df (m)	Fs	% Fs Effect of Geotextlle	% Fs Effect of Su Reduced
A 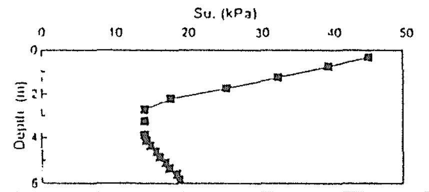	0	10.7	5.3	1.008	9.4	0.0
	0.2	10.7	5.3	1.030	11.8	0.0
	0.5	11.0	5.4	1.055	14.5	0.0
	1	11.8	5.3	1.070	16.2	0.0
	No reinf.	9.1	4.8	0.921	0.0	0.0
B 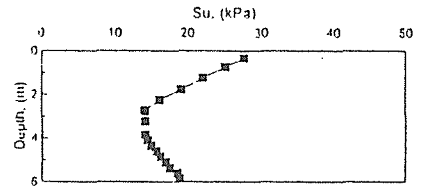	0	9.6	5.0	0.931	10.8	7.6
	0.2	9.7	5.0	0.959	14.2	6.9
	0.5	10.8	5.0	0.986	17.4	6.5
	1	11.3	5.3	1.003	19.4	6.3
	No reinf.	8.8	4.5	0.840	0.0	8.8
C 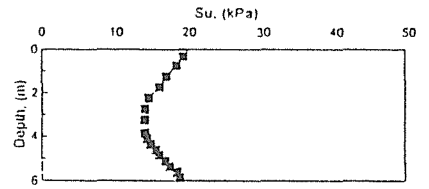	0	9.0	4.7	0.889	11.8	11.8
	0.2	9.3	4.8	0.920	15.7	10.7
	0.5	10.6	5.0	0.949	19.4	10.0
	1	11.3	4.8	0.966	21.5	9.7
	No reinf.	8.8	4.4	0.795	0.0	13.7
D 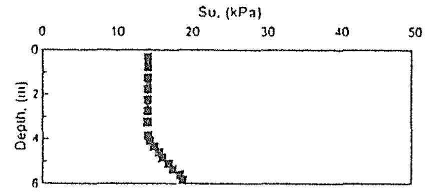	0	9.0	4.7	0.876	13.2	13.1
	0.2	9.0	4.7	0.906	17.1	12.0
	0.5	11.1	4.8	0.938	21.2	11.1
	1	11.3	4.8	0.954	23.3	10.8
	No reinf.	8.3	4.2	0.774	0.0	16.0
E 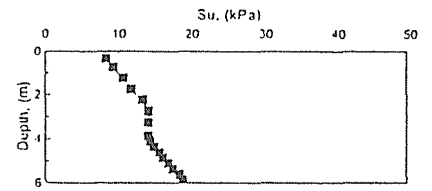	0	9.0	4.7	0.848	14.4	15.9
	0.2	9.0	4.7	0.879	18.6	14.7
	0.5	9.8	4.5	0.909	22.7	13.8
	1	10.5	4.8	0.927	25.1	13.4
	No reinf.	8.0	4.0	0.741	0.0	19.5
F 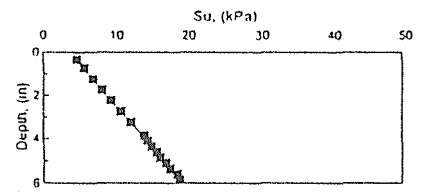	0	8.1	3.8	0.746	20.9	26.0
	0.2	8.1	3.8	0.778	26.1	24.5
	0.5	8.7	3.8	0.814	31.9	22.8
	1	9.7	3.8	0.834	35.2	22.1
	No reinf.	8.4	3.8	0.617	0.0	33.0

Where: If = Inclination factor of reinforcement force direction; Df = Potential failure depth
r = Radius; Fs = Factor of safety
% Fs Effect of Geotextile = 100 {(Fs) reinf. - (Fs) unreinf.}/ (Fs) unreinf.
% Fs Effect of Su Reduced = 100 {(Fs) A - (Fs) n}/ (Fs) A.

stress distribution of Test Facility II shows an expanded larger area with lesser concentration.

7. Effects of the Weathered Crust Layer

From the recent work of Koh (1995), six types of undrained strengths distributions of the foundation subsoils were analyzed as shown in Table 3. The site conditions for both Test Facility I and Test Facility II correspond to case A in Table 3. The analyses were made with respect to the stability of reinforced mass. When the strength of the topmost crust layer was reduced from case A to case F, the factor of safety against stability was reduced significantly. Moreover, the effect of reinforcements on the stability was more enhanced with reducing crust strength. Furthermore, it was found to be more efficient to use higher stiffness reinforcement when strong crust layer is present. Finally, it was found that the critical slip circle location and its radius tend to be smaller when the strength of the crust is reduced. Thus, either the presence of crust layer or utilization of reinforcements have potential to be effective only when the extent of the soft foundation is limited relative to the reinforced embankment dimensions.

8. Conclusions

Two test facilities were constructed to about 6.0m high with vertical facing, one with steel grids reinforcements (Test Facility I) and the other with polymer geogrid reinforcements (Test Facility II). Comparisons were made on their behavior in this study. Based on the results of the analyses, the following conclusions can be made:

1) The increase rigidity and stiffness of the reinforced mass tend to increase the settlement below the toe due to its rigid body rotation.
2) Increased rigidity and stiffness of the reinforced mass lead to lower lateral movements in the soft clay foundation subsoil.
3) Higher shear stress concentrations were observed beneath the toe of Test Facility I with inextensible reinforcements.
4) The locations of maximum tensile stress in the reinforcements tend to be nearer to the wall face than the conventional assumptions of coherent gravity and tie-back wedge analyses with reinforced structures on competent foundation. This is blamed on the compressions of the subsoil foundations.
5) Higher tensile forces were observed near the base of the reinforced mass due to the bending action resulting from bowl-shaped differential settlements.
6) The presence of strong crust as topmost layer of the soil profile affects the effectiveness of the reinforcements in improving the stability for the reinforced mass on soft foundation subsoil.

Acknowledgments

The authors expressed much gratitude and appreciation to the Institute of

Lowland Technology at Saga University, Japan for the financial support that made the conduct of this research work possible.

References

Alfaro, M. C. (1994). Reinforced Soil Wall/Embankment System on Soft Ground Using Inextensible and Extensible Grid Reinforcements. A progress report submitted to the Department of Civil Engineering, Saga University, Japan.

Bergado, D. T., Shivashankar, R., Sampaco, C. L., Alfaro, M. C. and Anderson, L. R. (1991). Behavior of Welded Wire Wall with Poor Quality, Cohesive-Frictional Backfills on Soft Bangkok Clay: A Case Study. Canadian Geotechnical Journal, Vol. 28, No. 6, pp. 860-880.

Koh, C. C. (1995). Design Guidelines for Geotextile Reinforced Embankments on Soft Clay Based on Full Scale Tests. M. Eng. Thesis, Asian Inst. of Tech., Bangkok, Thailand.

Tatsouka, F. (1992). Roles of Facing Rigidity in Soil Reinforcement. Proc. Intl. Symp. on Earth Reinforcement Practice, Vol. 2, Fukuoka, Japan, pp. 831-870.

著者略歴

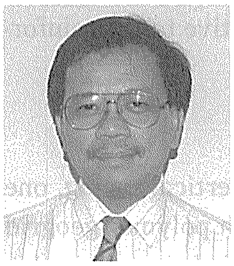

Dennes T. Bergado

1982年　ユタ州立大学博士課程修了
1982年　アジア工科大学助教授
工学博士

Marolo C. Alfaro

1988年　アジア工科大学修士課程修了
1988年　同上助手
1993年　佐賀大学大学院博士後期課程在学中

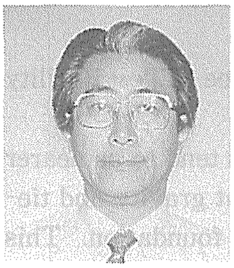

三浦　哲彦
(みうら　のりひこ)

1963年　九州大学卒業
1984年　佐賀大学教授
1991年　低平地防災研究センター長（併任）
1994年　佐賀大学理工学部長（併任）
工学博士